

# MUON BEAM EMITTANCE EVOLUTION IN THE HELICAL IONIZATION COOLING CHANNEL FOR BRIGHT MUON SOURCES \*

K. Yonehara<sup>†</sup>, C. Yoshikawa, Fermilab, Batavia, IL 60510, USA

Ya.S. Derbenev, A. Sy, JLab, Newport News, VA, USA

C. Ankenbrandt, R.P. Johnson, S.A. Kahn, Muons, Inc., Batavia, IL 60510, USA

B. Freemire, IIT, Chicago, IL, USA

M. Chung, UNIST, Ulsan 689-798, Korea

## Abstract

Characteristic of a helical lattice for six dimensional muon ionization cooling will be presented to utilize for a bright muon source. The beta function and the dispersion in the lattice are tunable by adjusting the helical magnetic component. As a result, the cooling decrements and the equilibrium beam emittance in transverse and longitudinal phase spaces are flexible. A helical magnetic component can be adjusted by changing the geometry of helical solenoid magnets. Manipulating a cooling path is an important capability in a bright muon source to serve a high quality muon beam for various muon beam applications.

## INTRODUCTION

A bright muon source is an ultimate tool to realize precise measurements in high-energy particle experiments. Muons are a true elementary particle, hence background events in  $\mu^+\mu^-$  collisions are significantly less complicated than hadron colliders. Since muons are 200 times heavier than electrons they can be accelerated to a multi-TeV energy without any synchrotron-radiation losses. Beamstrahlung is negligible in high energy  $\mu^+\mu^-$  collisions, hence the energy spread in a multi-TeV muon collider is significantly narrower than that in electron-positron collisions. The s-channel Higgs boson production rate in  $\mu^+\mu^-$  collisions is 40,000 times larger than in electron-positron colliders ( $\sigma_{Higgs} \propto m_{1+1}^2$ ). Thus, a muon collider Higgs factory is the only machine that can directly measure the mass width of Higgs bosons. Besides, a high energy muon storage ring provides an intense monochromatic neutrino beam.

Since muons are a tertiary particle the initial muon beam temperature after pion decays is too hot to admit the beam into the conventional accelerator complex. The beam should be cooled down to adequate temperature for a muon accelerator complex within a muon life time. To achieve fast cooling, a helical muon six-dimensional (6D) phase space ionization Cooling Channel (HCC) is proposed. Theoretically, the 6D beam volume can be reduced  $10^6$  in a 300 m-long HCC. It consists of a high-pressure  $H_2$  gas-filled helical RF system which is incorporated into a helical magnet. Gas in the RF cavities acts as not only an ionization cooling matter but also buffering dark currents to achieve high RF gradients in

multi-Tesla fields. The helical magnetic component is generated by using a helical solenoid coil. Since the HCC lattice is a continuous structure there is no betatron resonance. It realizes a huge momentum acceptance.

The helical solenoid coil is flexible to tune the beta function and the dispersion by adjusting the geometry of coil and adding the correction magnet [1]. The lattice parameters are the key to manipulate the cooling decrements and the equilibrium emittance in transverse and longitudinal phase spaces. We demonstrate the theoretical predictions for the phase space mapping to design the cooling path and a numerical evaluation at the specific cooling condition for conceptual design of the HCC.

## FLEXIBILITY OF HCC

The HCC linear theory in a homogeneous cooling matter was derived by Derbenev and Johnson [2]. The theory was confirmed by comparing with various numerical results [3–5]. Figures 1 and 2 show the validation of HCC theory. We used G4Beamline in the simulation effort [6].  $H_2$  gas pressure is 160 atm at room temperature and 20  $60\mu\text{m}$ -thick- $Be$  RF windows per meter are equally distributed on the beam path. According to the theory, the transverse betatron

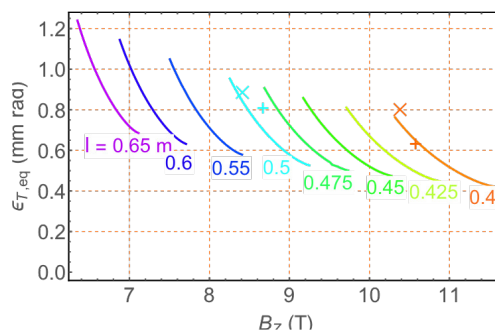


Figure 1: Prediction (a solid line) and the numerical result (a cross mark) of the transverse equilibrium emittance. Values in the plot represents the helical period,  $\lambda$ .

function,  $\hat{\beta}_T$  is characterized by the helical period,  $\lambda$  and the solenoidal field strength,  $B_z$ , i.e.  $\hat{\beta}_T$  is lower in shorter  $\lambda$  and/or stronger  $B_z$ . Therefore, lower equilibrium  $\epsilon_T$  is made at shorter  $\lambda$  and/or stronger  $B_z$  and vice versa. On the other hand, the longitudinal betatron function,  $\hat{\beta}_L$  is characterized by a momentum slip factor,  $\eta$  which is given by the dispersion,  $D$ . According to the theory,  $D$  becomes closer to the energy transition, i.e.  $\eta \sim 0$  (isochronous) in stronger

\* Work supported by Fermilab Research Alliance, LLC under Contract No. DE-AC02-07CH11359 and DOE STTR grant DE-SC0007634

<sup>†</sup> yonehara@fnal.gov

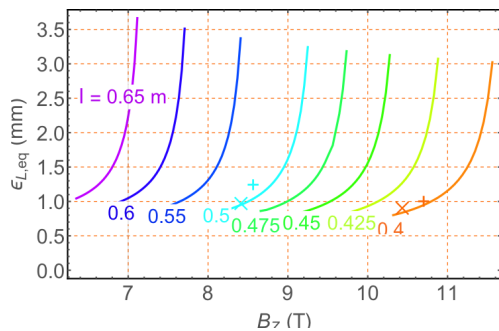


Figure 2: Prediction (a solid line) and the numerical result (a cross mark) of the longitudinal equilibrium emittance. Values in the plot represents the helical period,  $\lambda$ .

$B_z$ . Consequently,  $\hat{\beta}_L$  becomes longer in stronger  $B_z$ , hence lower equilibrium  $\varepsilon_L$  is made at stronger  $B_z$ . Note that the RF bucket size is infinite at  $\eta = 0$ , hence the longitudinal admittance is bigger at stronger  $B_z$ . It is demonstrated in Fig.7 in ref. [4]. The equilibrium 6D emittance is determined by the energy loss rate and  $B_z$ . Because  $\varepsilon_{6D} \sim \varepsilon_T^2 \times \varepsilon_L$  a low- $\varepsilon_T$  configuration makes a high- $\varepsilon_L$  and vice versa.

The studies also demonstrate how the equilibrium emittance can be manipulated by the helical lattice. A longitudinal cold muon beam can be generated by tuning  $D$  even at long  $\lambda$ , i.e. muon energy spread,  $\Delta E$  reaches 4.5 MeV at the design momentum 200 MeV/c. Especially, a longitudinal cold beam is required for a muon collider Higgs factory, g-2 and Mu2e experiments. Recently, a skew-quad parametric resonance ionization cooling (PIC) channel was proposed for extra transverse cooling [7]. By combining the longitudinal cold HCC with the PIC we could produce the extremely cold 6D muon beam.

## MATCHING DESIGN

The HCC operates above transition, while the linear systems upstream (phase-rotator and initial cooler) run below it. Hence, transition must be crossed in matching into the HCC. An adiabatic approach was originally considered, but non-linear dynamics imposed on a beam with large phase space caused too much beam loss and motivated a complimentary method to jump transition immediately from the straight channel upstream directly into the HCC as shown in Figure3 with resulting matching efficiency of 80 % [8]. Advances in understanding and controlling non-linear dynamics in the future may warrant a revisit of the adiabatic approach.

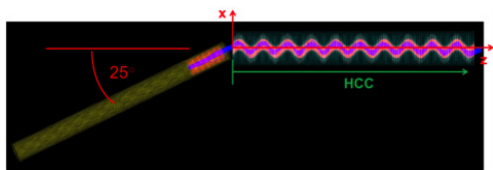


Figure 3: Top view of match into HCC (RF and  $H_2$  gas removed).

## COOL INTENSE MUON BEAM

Possible issues with intense muon beam in the HCC will be discussed. Two beam conditions are considered: A muon beam is bunched and the total intensity exceeds  $10^{13}$  muons/spill. Or, a muon beam is single bunch but the beam density exceeds  $\sim 10^{14}$  muons/cm<sup>3</sup>. There is no beam intensity effect below these quantities.

### Plasma Loading Effect

Most critical issue is the plasma loading effect in the gas-filled helical RF system. The ion pairs in a beam-induced gas plasma consume the RF power in the cavity. The amount of ion pairs are accumulated with quadratic as a function of the bunch number in a bunch train. The plasma dynamics was investigated to mitigate the plasma loading. We found that a small amount of electronegative dopant was significantly improve the plasma loading.

Figure 4 shows the estimated RF voltage for the final bunched beam in a bunch train beam. The RF voltage is down to 90 % with a typical muon collider beam,  $10^{12}$  muons/bunch. Detail beam condition is presented in ref. [9].

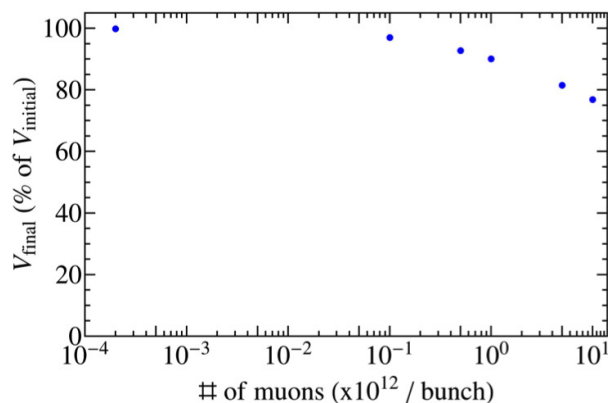


Figure 4: Estimate RF voltage drop due to the plasma loading in a 650 MHz gas-filled pillbox cell.

### Peak RF Gradient Dependence

The beam loading has been studied in analytical method [10, 11]. As we mentioned in the plasma loading, the beam loading is also critical with a bunched beam. Detailed description can be found in ref. [11].

The acceptable RF gradient drop in the HCC has been investigated in numerical simulation to involve the plasma and the beam loading effects. The gas pressure is 160 atm and 20  $60\mu\text{m}$ -thick- $Be$  RF windows per meter are equally distributed in this analysis, hence the average energy loss is 9.0 MeV/m at  $p = 200$  MeV/c. The RF gradient will be dropped by 10~40 % at the total number of muons  $10^{13}$  which corresponds to 18~12 MV/m with the design RF gradient 20 MV/m [11].

Figure 5 shows the evaluated transmission efficiency in the HCC ( $\lambda = 0.4$  m,  $\kappa = 1.0$ ) as a function of the peak

RF gradient in G4Beamline. In order to recover the energy loss in the channel, the synchrotron phase is tuned for each gradient, but the helical lattice is the same. The transmission efficiency is suddenly dropped to zero at the peak RF gradient 14 MV/m. One possible lost mechanism is smaller RF bucket size with lower longitudinal focusing. The RF bucket size at the peak RF gradient 14 MV/m is 2.5 times smaller than the design gradient. Muons are fell off from the RF bucket.

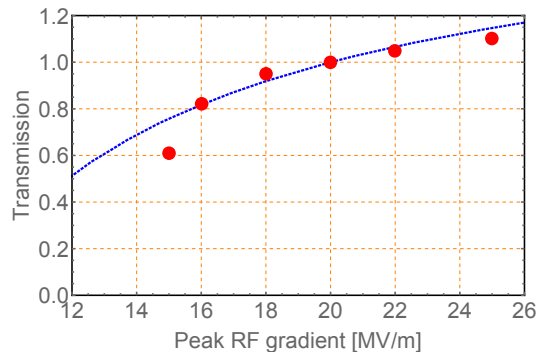


Figure 5: Evaluated transmission efficiency in the HCC as a function of peak RF gradient. A red point is the simulation result. A blue dotted line is the prediction from eq.(8) in ref. [5].

### Space Charge Effect

The space charge effect in the HCC has also been investigated. The transverse oscillation equation including with the tune shift is given by using a uniform KV beam model,

$$\frac{d^2 r_b}{ds^2} + \left( \kappa_{sf} - \frac{K_b}{r_b^2} \right) r_b = \frac{\varepsilon_{KV}^2}{r_b^3}, \quad (1)$$

where  $r_b$  is the radius of beam size,  $\kappa_{sf}$  is a focal strength of the lattice,  $K_b$  is the transverse space charge force, and  $\varepsilon_{KV}$  is a transverse emittance, respectively. The calculation shows that the space charge effect is negligible up to  $10^{14}$  muons/cm<sup>3</sup> at the normalized transverse emittance 300  $\mu$ m, the rms beam size 2 mm, and the rms bunch length 2 cm.

On the other hand, the longitudinal space charge effect is given the similar equations,

$$\frac{d^2 z_m}{ds^2} + \left( \kappa_z - \frac{K_L}{z_m^3} \right) z_m = \frac{\varepsilon_{zz'}^2}{z_m^3}, \quad (2)$$

where  $z_m$  the bunch length,  $\kappa_z$  is the longitudinal focal strength,  $K_L$  is the longitudinal space charge force, and  $\varepsilon_{zz'}$  is a longitudinal emittance, respectively. The longitudinal emittance will be changed by 1.6 at  $10^{14}$  muons/cm<sup>3</sup> with the normalized longitudinal emittance is 1 mm and the rms bunch length is 2 cm. This makes an impact on a solenoid based cooling channel, e.g. a rectilinear FOFO channel since it has a below transition ( $\eta < 0$ ). Therefore, the final longitudinal emittance grows 1.6 that is good agreement with the

numerical simulation [12]. In case of the HCC, the longitudinal space charge becomes the focus effect. Therefore, the final emittance can be smaller than the present simulation result. Further numerical study involving the space charge effect is needed.

### Beam-plasma Interaction

A beam-plasma interaction is other possible issue in gas-filled RF cavities with intense muon beams. Since single incident muon generates  $\sim 2,000$  ion pairs/cm in a 160 atm  $H_2$  gas the small fraction of the collective effect in the beam-induced plasma changes the electromagnetic field distribution in the beam bunch. Indeed, the weak field generated by incident muon beam induces the plasma oscillation and makes the charge neutralization of the incident beam. Detail numerical evaluation has been done [13].

### REFERENCES

- [1] K. Melconian et al., "Alternative Methods for Field Corrections in Helical Solenoids" IPAC'15, Richmond, USA, June 2014, WEPTY059 (2015).
- [2] S. Derbenev, R.P. Johnson, Phys. Rev. ST Accel. Beams 8, 041002 (2005).
- [3] K. Yonehara et al., "Simulations of a Gas-Filled Helical Muon Beam Cooling Channel", PAC'05, Knoxville, Tennessee, TPPP052 (2005).
- [4] K. Yonehara, "Study Cooling Performance in a Helical Cooling Channel for Muon Colliders", IPAC'14, Dresden, Germany, June 2014, TUPME014 (2014).
- [5] K. Yonehara, "Study Cooling Performance in a Helical Cooling Channel for Muon Colliders", IPAC'14, Dresden, Germany, June 2014, TUPME015 (2014).
- [6] T.J. Roberts, <http://www.muonsinternal.com/muons3/G4beamline>
- [7] A. Afanasev et al., "Skew-Quad Parametric-Resonance Ionization Cooling: Theory and Modeling", IPAC'15, Richmond, USA, June 2014, TUPHA013 (2015).
- [8] C. Yoshikawa et al., "Status of the Complete Muon Cooling Channel Design and Simulation", IPAC'14, Dresden, Germany, June 2014, TUPME016(2014).
- [9] B. Freemire et al., "High Pressure Gas-Filled RF Cavities for Use in a Muon Cooling Channel", NAPAC'13, Pasadena, CA, USA, TUODA1 (2013).
- [10] M. Chung et al., "Effects of Beam Loading and Higher-order Modes in RF Cavities for Muon Ionization Cooling", IPAC'14, Dresden, Germany, June 2014, THPRI065 (2014).
- [11] M. Chung et al., "Transient Beam Loading Effects in Gas-filled RF Cavities for a Muon Collider", IPAC'14, Dresden, Germany, June 2014, THPRI053 (2014).
- [12] D. Stratakis et al., Phys. Rev. ST Accel. Beams 18, 044201 (2015).
- [13] J. Ellison et al., "Beam-Plasma Effects in Muon Ionization Cooling Lattices", IPAC'15, Richmond, USA, June 2014, WEPWA063 (2015).